Tectono-Sequence Stratigraphic Interpretation of Late Miocene to Early Pliocene Deposits of Shallow Offshore, Niger Delta*

Norbert Ajaegwu[1], Berthrand Ozumba[2], Izuchukwu Obiadi[1], Emmanuel Anakwuba[1], David Anomneze[1], Gabriel Okeugo[3], and Charles Ugwueze[4]

Search and Discovery Article #20246 (2014)
Posted April 14, 2014

*Adapted from extended abstract prepared in conjunction with oral presentation at AAPG 2014 Annual Convention and Exhibition, Houston, Texas, April 6-9, 2014,

[1]Geological Sciences, Nnamdi Azikiwe University, Awka, Anambra State, Nigeria (ajejike@yahoo.com)
[2]Geological Services, Shell Petroleum Development Company Limited, Port Harcourt, Rivers State, Nigeria
[3]Geology, University of Nigeria, Nsukka, Enugu State, Nigeria
[4]Geology, University of Port Harcourt, Rivers State, Nigeria

Abstract

This study documents the regional stratigraphic framework and structural configurations of three blocks, H, J and K located in the Shallow Offshore of the Niger Delta. The purpose of this study is to use sequence stratigraphic framework, seismic facies and geomorphology and structural configuration as tools for prediction of reservoir distributions in relation to structuration. The dataset consists of a 3-D seismic volume, wireline log suites (gamma ray, resistivity and sonic), biofacies, palynological and foraminiferal biozones and a Niger Delta chronostratigraphic chart.

A total of 15 wells drilled in these blocks within the last twenty years were studied. The ages (Ma) of the maximum flooding surfaces identified a range from 3.9-11.5 Ma, while that of the sequence boundaries range from 4.1-10.6 Ma. On strike there was a variation in the number of sequences from three to five and correlated wells tended to be older and shallower in paleobathymetry eastward.

Flattening at 5.0 Ma (Upper Messinian) (maximum flooding surface above 5.6 Ma sequence boundary) shows that at the proximal portion, the system tracts gradually thin eastward showing that the rate of creation of accommodation increases westward. We attribute the increase in accommodation westward to the structural configuration of the area which allowed the formation of collapsed crest structures in the H Block while the eastward decrease in accommodation is associated with closely spaced flank faults informally called the K faults in the K Block. At the distal portion, the correlation shows that individual system tracts thickened at the centre and thinned at the flanks. We interpreted this

feature as channels in seismic with concave upward geometry at the centre with the thickened centre representing an incised valley created during base level fall at the 5.6 Ma sequence boundary which was filled at the next sea- level rise.

Six seismic facies were interpreted based on the reflection attributes. Among the six facies, the most favourable reservoir-seal pairs were established in mounded seismic facies. Good reservoir-seal pairs ensured that the mounded seismic facies all contained hydrocarbons and such facies should be targeted.

The geologic model showed that the study area could be divided into three macrostructures that control sediment accumulation in the area. The counter regional fault that demarcate FB I and FB II macrostructures appeared to exert major control on sediments accumulation by creating more accommodation in the hanging wall part.

Introduction

The Niger Delta Basin ranks amongst the world's most prolific petroleum producing Tertiary deltas that together account for about 5% of the world's oil and gas reserves and for about 2-5% of the present-day basin areas on Earth (Reijers et al., 1996). Well sections through the Niger Delta generally display three vertical lithofacies subdivisions, namely the Benin, the Agbada and the Akata formations corresponding to delta plain, delta front and prodelta respectively. The lithological characterizations of these lithostratigraphic units have been described by Short and Stauble (1967), Weber and Daukoru (1975), and Whiteman (1982). The Benin Formation consists of massive continental sands and gravels accounting for about 90% of all the lithofacies with few shale intercalations which become more abundant toward the base. The Agbada Formation consists mostly of shoreface and channel sands with minor shales in the upper part, and alternation of sands and shale in equal proportions in the lower part. Oil and gas reverses in the Niger Delta Basin mainly occur in sandstone reservoirs throughout the Agbada Formation. The Akata Formation is composed mainly of marine shales, sandy and silty beds, which are thought to have been laid down as turbidites and continental slope channel fills.

The H, J and K blocks situated within Oil Mining Lease (OML) 77, 74 and 72 respectively are located in the proximal portion of the Offshore Depobelt and referred to as the Shallow Offshore (Figure 1). Two strike lines running from H Block in the central part of offshore Niger Delta, through J Block to K Block in the eastern part, were selected. A total of 15 wells drilled in these blocks within the last twenty years were studied. The summary of exploration activities in the study area over the years is presented as Figure 2.

Methodology

The methods employed in carrying out this work are as followed: first the sequence stratigraphic framework was built and various correlations were performed using the Petrel platform. In building the sequence stratigraphic framework, we made use of biozones, biofacies/paleobathymetry, abundance and diversity plots of forams and wireline logs (gamma ray, resistivity and sonic). The Niger Delta Chronostratigrapic Chart (Figure 3) serves as a guide in assigning ages to key stratigraphic surfaces such as Maximum Flooding Surfaces (MFSs) and Sequence Boundaries (SBs). Key sequence stratigraphic surfaces and reservoir thicknesses were correlated across wells. Secondly, structural and stratigraphic surfaces (MFS and SB) interpretations were performed on a 3-D seismic volume

(hblk_2013:9_13_PSDM_FULL_T_/NFLT) using nDI Geosign software. Time-depth conversion was done to enable conversion of time structure maps to depth structure maps. Thirdly, seismic facies and geomorphology were interpreted in order to delineate the lithofacies distributions, environments of deposition and possible channel depositional lobes. Finally, the stratigraphic and structural models were integrated to build geologic models using the Petrel platform. From the geologic model, the play concept was evaluated.

Results and Discussion

Correlation of Key Surfaces and Reservoirs

Based on the positions of the wells, two strike lines, namely 1 and 2, have been chosen for well to well correlations. The strike line 1 cuts across wells that lie below strike line 2. The correlation was based on the interpreted stratigraphic surfaces (MFS which ranges from 11.5 Ma and SB ranging from 10.6 Ma to 4.1 Ma) and reservoir thickness.

Observations of the correlations across the two strike lines showed that:

1) On strike, there was a variation in the number of genetic sequences from three to five.

2) At the proximal part (strike line 2), the system tracts tend to thin eastward, while at the distal part (strike line 2) the system tracts thickened at the centre and thin at the flanks within 5.6 Ma SB and 5.0 Ma MFS (Figure 3.1).

3) At the proximal portion, the sand packages (reservoirs) pinch out toward the east, while at the distal portion they thickened at the centre and thin at the flanks within the same chronostratigraphic framework (Figure 3.2).

4) The wells gradually become older eastward.

To understand these observations, we decided to flatten at 5.0 Ma. The observed trends are shown in Figure 3.3. The essence of flattening is to remove tectonic effects and assume a common datum. The trend of thickening at the centre and thinning at the flanks is consistent with stratigraphic surfaces and reservoir thickness correlation panels as shown previously in Figure 3.1 and Figure 3.2. The challenge is to explain the sudden thickening at the centre and thinning at the flanks of the distal portion of the study area.

Structural Interpretation

Structural interpretation showed that both J and H blocks are affected by collapsed crest structures, while the K Block is mainly typified by closely spaced flank faults, informally called K-faults by Evamy et al. (1968) (Figure 4). The implication of collapsed crestal structures is that they create more accommodation for sediment accumulation. Projection of interpreted seismic data onto the stratigraphic framework flattened at Upper Messinian (5.0 Ma) surface at the distal section (strike line 1) showed that the thickened section is within the collapsed crest structure (Figure 5). However, within JK Field in J Block, the sequence is thicker compared to both H and K blocks at the flank. The thickened section is

interpreted to be an incised valley created by base level fall at 5.6 Ma SB. This valley was filled during the subsequent healing stage (transgression) as sea-level rises.

Fault and Horizon Interpretation

The fault picking was done on a grid of 64 along tracks in traverse view using nDI GeoSign software with help of a semblance map. Three surfaces comprising 5.0 Ma MFS, 5.6 Ma SB and 6.0 Ma MFS were interpreted on the seismic.

Seismic Facies Interpretation/Classifications

Six seismic facies were identified based on reflection configuration, amplitude, frequency and lateral and vertical bounding relationships with other reflectors. The reference scheme used are those of Brown and Fisher (1984), and Janson et al. (2011).The reflection attributes used in defining each of these listed seismic facies were illustrated in shown in Figure 6 while their calibrations with well information are shown in Figure 7.

The parallel, continuous configuration suggests uniform sedimentation conditions, while a wavy continuous configuration suggests a sequence deposited on top of a subsiding substratum. Well information shows that both parallel and wavy continuous configurations are associated with channel sandstone. However, both possess poor reservoir-seal pairs and may hold little or no hydrocarbons. The oblique, discontinuous, low amplitude facies were interpreted as shallow marine progradation in a high energy environment.

The mounded chaotic and continuous, low amplitude facies showed good reservoir-seal pairs which ensured that the facies all contained hydrocarbons. These facies are found towards the western portion of the study area within the H Block. The mounded, chaotic facies were interpreted to occur at the shelf edge (lower shelf environment), while mounded, continuous facies suggested deposition within the slope. From the positions of the wells, interpreted paleobathymetry and seismic facies (mounded, continuous, low amplitude), the slope deposits appear to have started around HA-001 well and move basinward toward the western flank (HB-001 and Hobobo-001 wells).

Seismic Geomorphology

Seismic geomorphology, when used in conjunction with seismic stratigraphy, represents the state of the art approach to extracting stratigraphic insights from 3-D seismic data (Posamentier et al., 2007; Reijenstein et al., 2011).

The interpretation was done on a .vt file using sculpting attribute in the nDI GeoSign software environment. Both horizon and proportional slicing was carried out and viewed on both peak and trough. The 5.0 Ma MFS time structure map (isochron) was used for horizon slicing. The implication of horizon slicing is that events are flattened at a particular surface while slicing at a chosen interval. The slicing was done at every 20 msecs starting at zero offset. At 4.0 msecs offset, the channel sands saddled by JN Field were clearly shown on the sculpted volume (Figure 8). With the application of proportional slicing, we started seeing some plan view images that resemble depositional environments. At 4.4 msecs window and using 5.0 Ma MFS surface as upper surface and 5.6 Ma SB surface as lower surface, one of the channels appeared on the

sculpted volume running in the north-south direction. This channel developed into fans forming a depositional lobe towards the JK Field (Figure 9) and this depositional lobe could be supplying sediments to JK Field.

Geologic Model

The 3-D static model was built by integrating structural, stratigraphic and lithological interpretations in the study area. The structural model was produced by pillar gridding the selected faults and converting them to fault surfaces. The modelled faults were then aligned to the original faults in the depth structure maps to make sure that they maintain the original trend.

The stratigraphic model was built by interpreting reservoir tops and bases above and below three interpreted surfaces (5.0 Ma MFS, 5.6 Ma SB and 6.0 Ma MFS) and correlating them across the wells. These reservoir tops and bases were converted to isochors (thickness maps). The stacked isochores were layered to accommodate both reservoirs and the shales. The integrated model is shown as geologic model in Figure 10 below.

A closer look at the geologic model showed that two major down-to-basin growth faults (one synthetic boundary fault and one counter regional fault occurring toward the western portion) divide the study area into three macrostructures. These structures are named Fault Block I (FB I), Fault Block II (FB II) and Fault Block III (FB III). FB I houses the HB, Hobobo and HA fields, the FB II houses the HB, HM, HD and JK fields, while the FB III houses the JO, JN and KF fields. The FB II contains series of grabens forming a collapsed crest structures. Sediments within one of the grabens bounded by the counter regional fault that demarcate FB I and FB II and stretched to an opposing fault just after HD Field are thicker compared to those in the flanks. These sediments are at the hanging wall of the counter regional fault. The implication is that this counter regional fault is the major fault that controls sediment accumulation in the area. The incised valley fill (IVF) around the JK Field clearly shows in the model; however, it appears to extend more in an eastern direction. This could be due to lack of well control between the JK and JN fields, which are wide apart.

Conclusion

This study has identified various incisions caused by base sea level fall at the 5.6 Ma and 6.7 Ma sequence boundaries and the associated channel systems. These sequence boundaries tend to incise on the underlying strata creating valleys, then these valleys are filled during retrogradation with good sands which make prospectivity robust in the area.

Seismic geomorphology shows that the depositional lobe of one of the channels is towards the incised valley. This lobe is in the form of a fan and could be supplying sediment to the valley.

Six seismic facies were interpreted based on the reflection attributes. Among the six facies, the most favourable reservoir-seal pairs were established in mounded seismic facies. Good reservoir-seal pairs ensured that the mounded seismic facies all contained hydrocarbons and such facies should be targeted.

The geologic model showed that the study area could be divided into three macrostructures that control sediment accumulation in the area. The counter regional fault that demarcates FB I and FB II macrostructures appears to exert major control on sediment accumulation by creating more accommodation in the hanging wall part.

References Cited

Brown Jr., L.F., and W.L. Fisher, 1984, Principles of seismic stratigraphic interpretation: interpretation of depositional systems and lithofacies from seismic data: AAPG Education Program, p.1-88.

Janson, X., C. Kerans, R. Loucks, M. AlfredoMarhx, C. Reyes, and F Murguia, 2011, Seismic architecture of a Lower Cretaceous platform-to-slope system, Santa Agueda and Poza Rica fields, Mexico: AAPG Bltn., v. 95/1, p. 105-146.

Posamentier, H.W., and P.R.Vail, 1988, Eustatic controls on clastic deposition II, Sequence and systems tract models, *in* C.K.Wilgus, B.S.Hastings, C.G. St. C. Kendall, H.W. Posamentier, C.A. Ross, and J.C. Van Wagoner, eds., Sea Level Changes - An Integrated Approach: Society for Sedimentary Geologists (SEPM) Special Publication 42, p. 125-154.

Reijenstein, H.M., H.W. Posamentier, and J.P. Bhattacharya, 2011, Seismic geomorphology and high-resolution seismic stratigraphy of inner-shelf fluvial, estuarine, deltaic, and marine sequences, Gulf of Thailand: AAPG Bltn., v. 95/11, p. 1959-1990.

Reijers, T.J.A., S.W. Petters, and C.S. Nwajide, 1996, The Niger Delta Basin, *in* T.J.A. Reijers, ed., Selected Chapters on Geology: SPDC Corporate Reprographic Services, Warri, Nigeria, p. 103-114.

Short, K.C., and A.J. Stauble, 1967, Outline of geology of Niger Delta: AAPG Bltn., v. 51/5, p. 764-772.

Weber, K.J., and E. Daukoru, 1975, Petroleum geology of the Niger Delta: 9th World Petroleum Congress Proceedings 2, p. 209-221.

Whiteman, A, 1982, Nigeria: Its petroleum geology, resources and potential: London, Graham & Trotman Ltd., v. 1, p. 131-132.

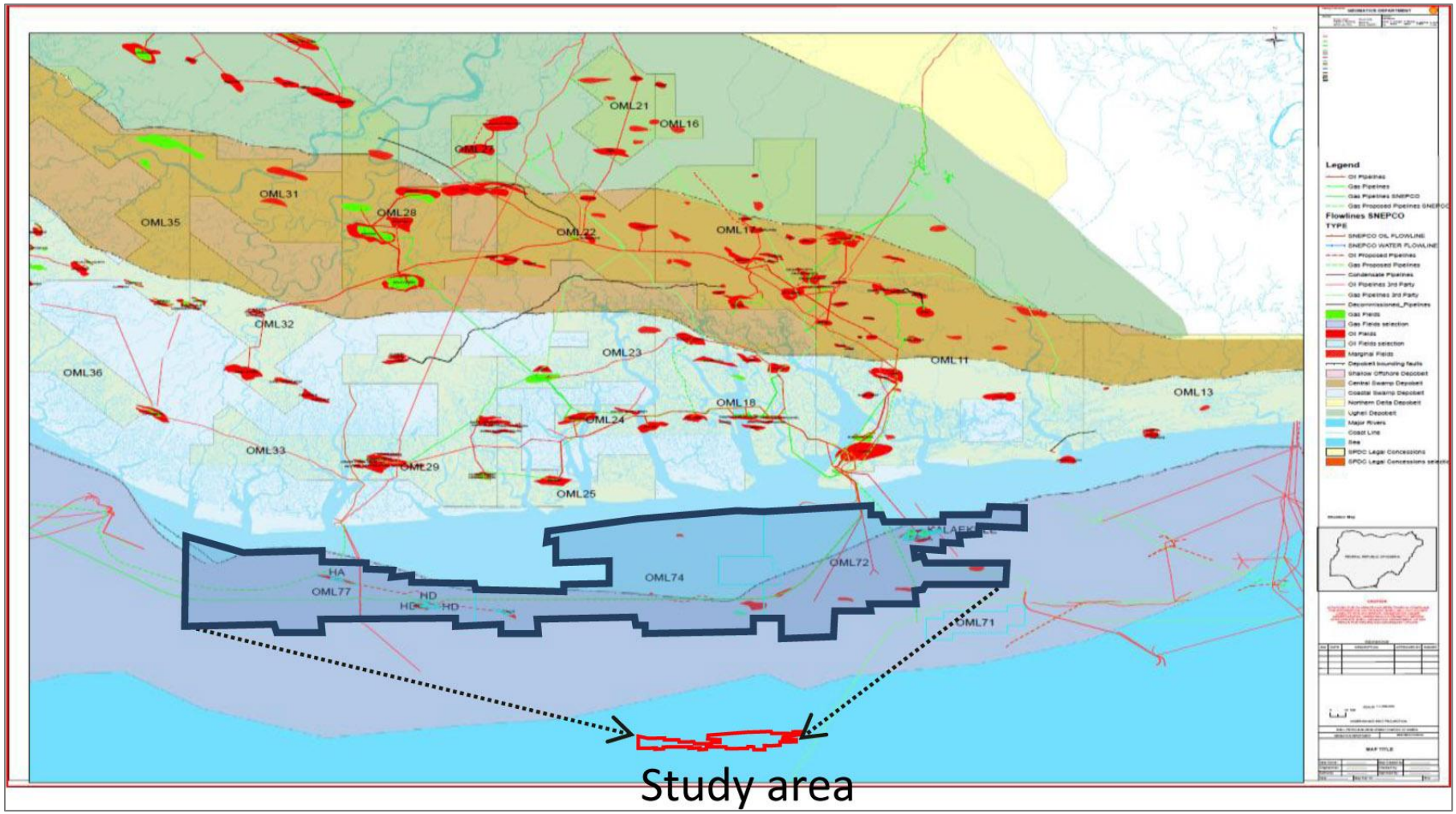

Figure 1. Location and infrastructure map of the study area.

Block (OML)	No. of wells drilled to date	Nature of Wells	Wells used for the study	Area coverage (sq. Km)
H (OML 77)	12 wells (between 1965 & 1989)	6 exploratory 6 appraisal	HD-001 HB-001 HA-001 HM-001 Hobo-001	962
J (OML 74)	9	3 marginal 2 mainly gas 3 dry hole 1 (2004) prolific: 60ft tvd oil	JO-001 JK-001 JK-002 JN-001	2, 130
K (OML 72)	43 (since 1964)	1 producing 6 partially appraised/ unappraised field 5 marginal field	Kapp-001 Kaue-001 Kora-003 KF-001 KI-001 KR-001	1, 245 (OML 72& 71)

Figure 2. Key statistics/summary table of study area.

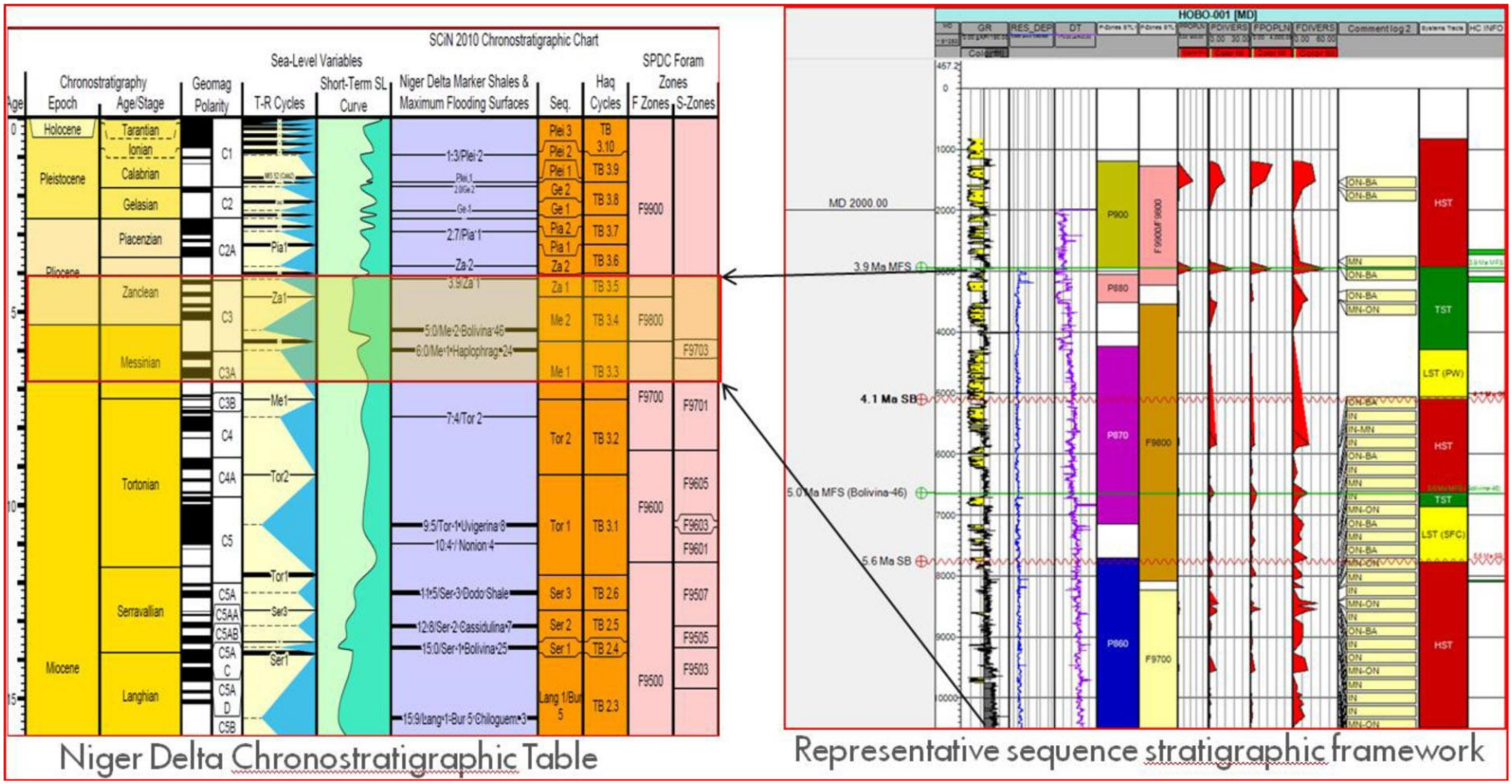

Figure 3. Representative sequence stratigraphic framework and comparative ages in the Niger Delta.

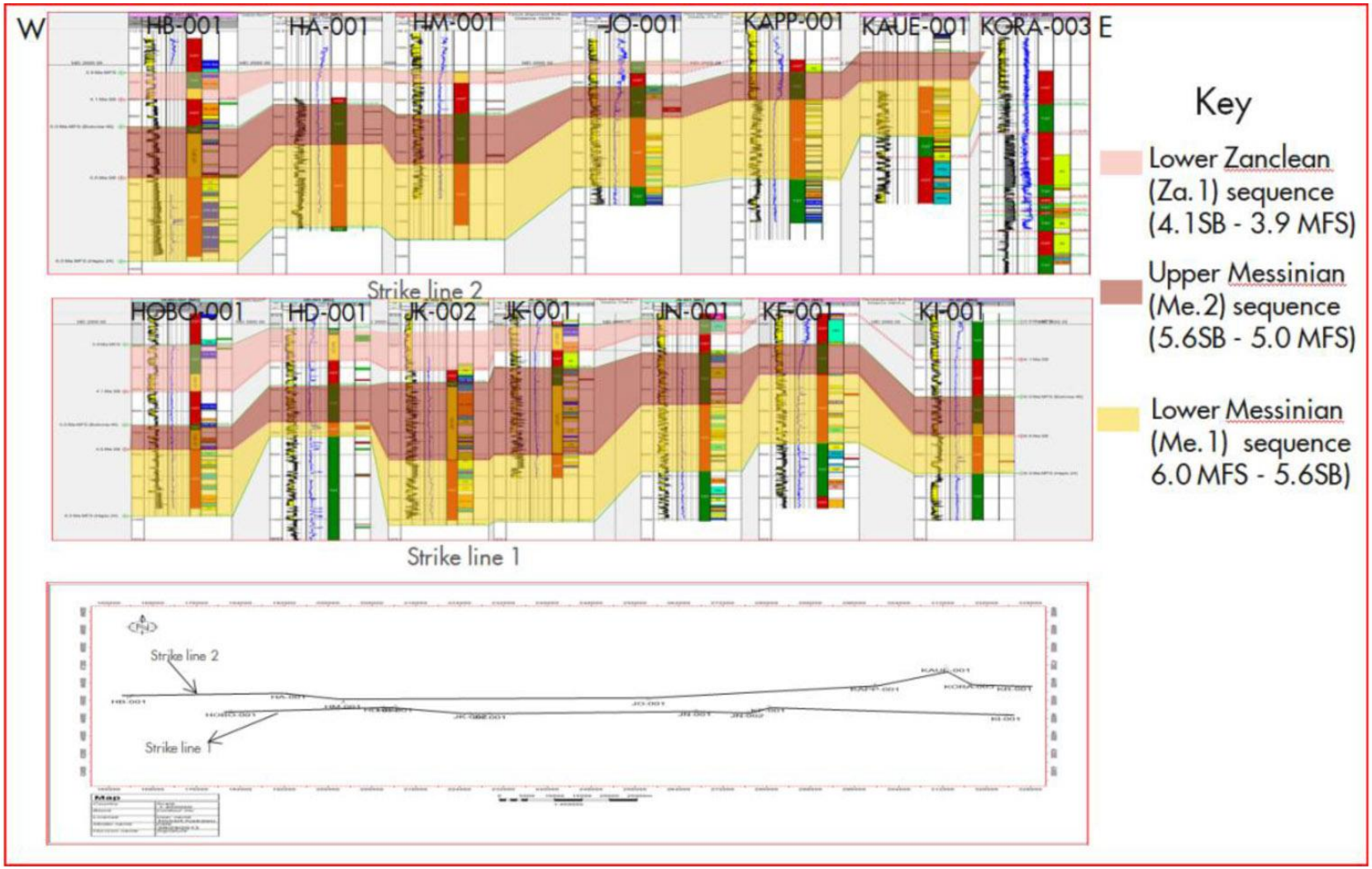

Figure 3.1. Correlated sequence stratigraphic surfaces across strike line 1 and 2.

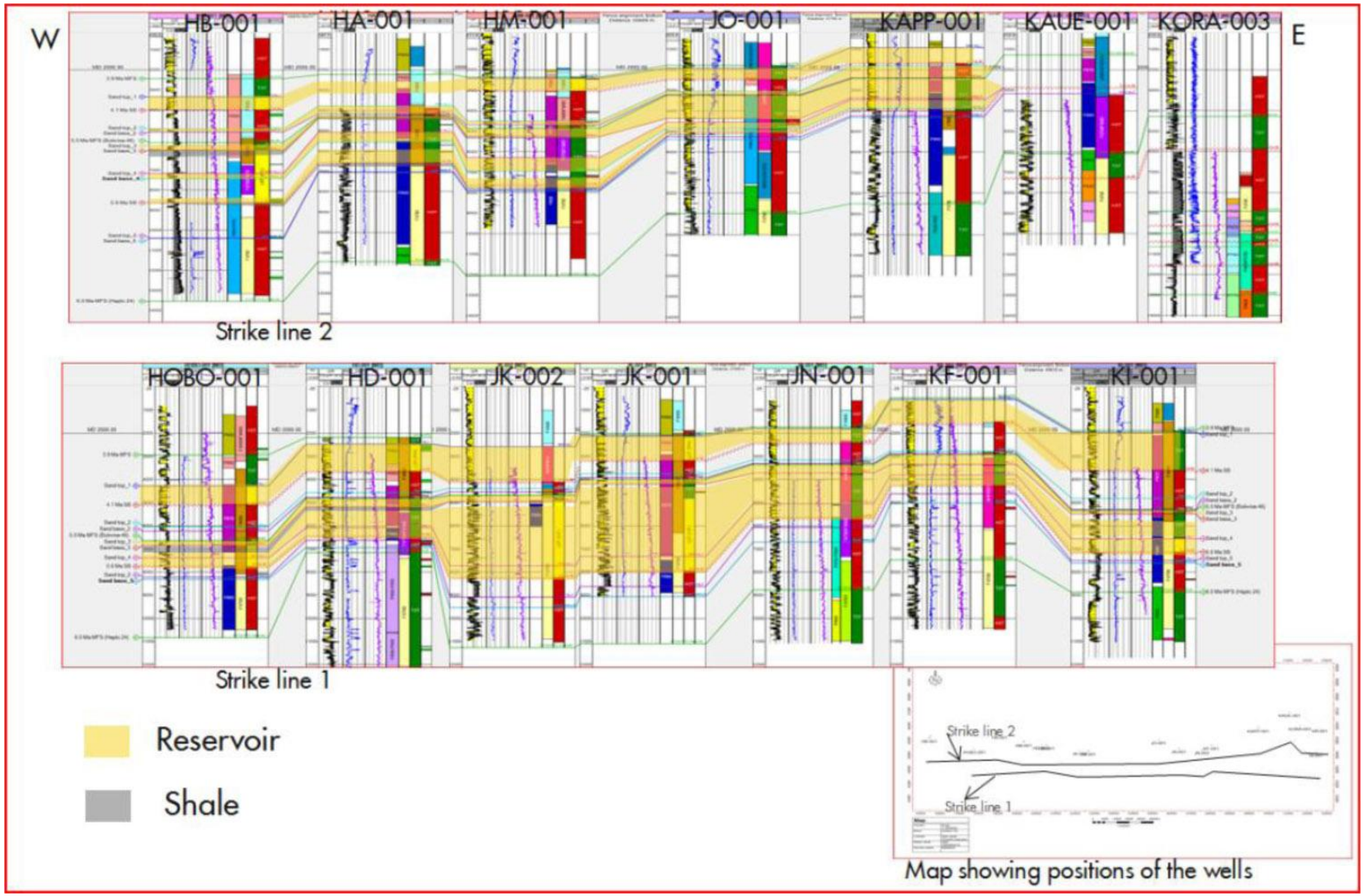

Figure 3.2. Reservoir thickness correlation across the two strike lines.

Figure 3.3. Event flattened at 5.0 Ma MFS across strike line 1 and 2.

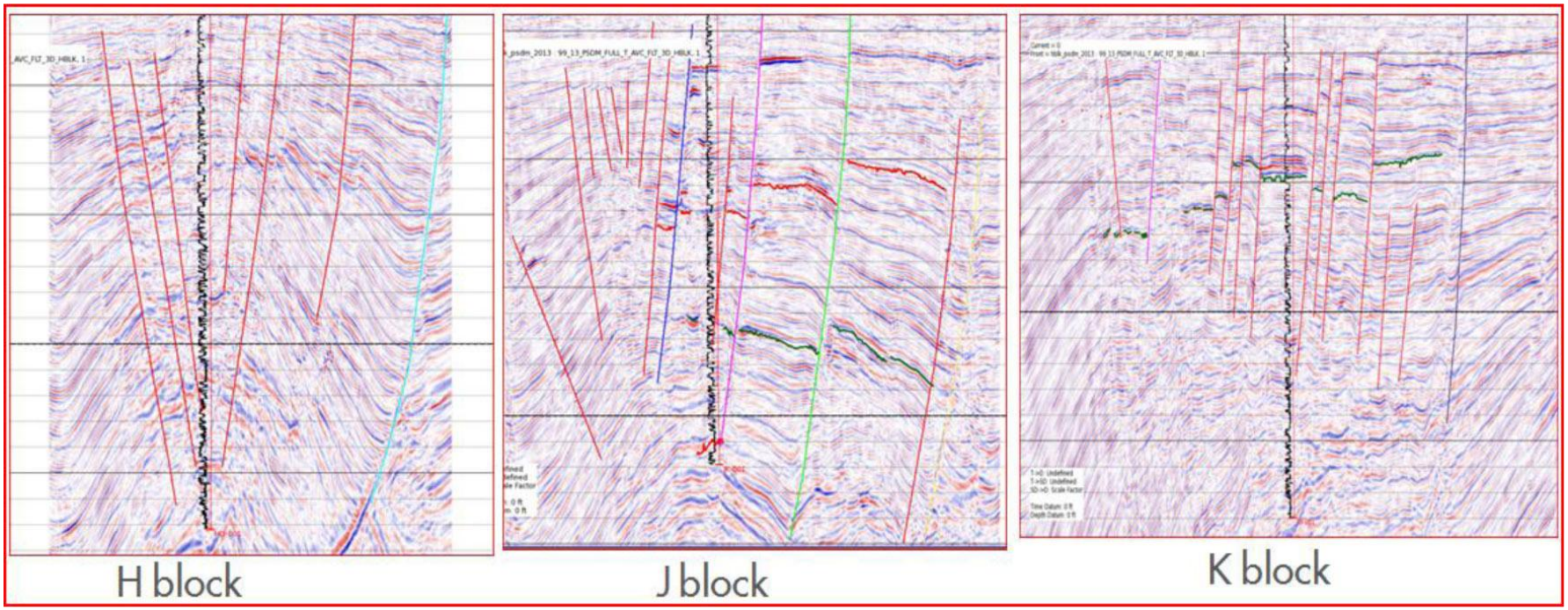

Figure 4. Structural configurations within H, J and K blocks.

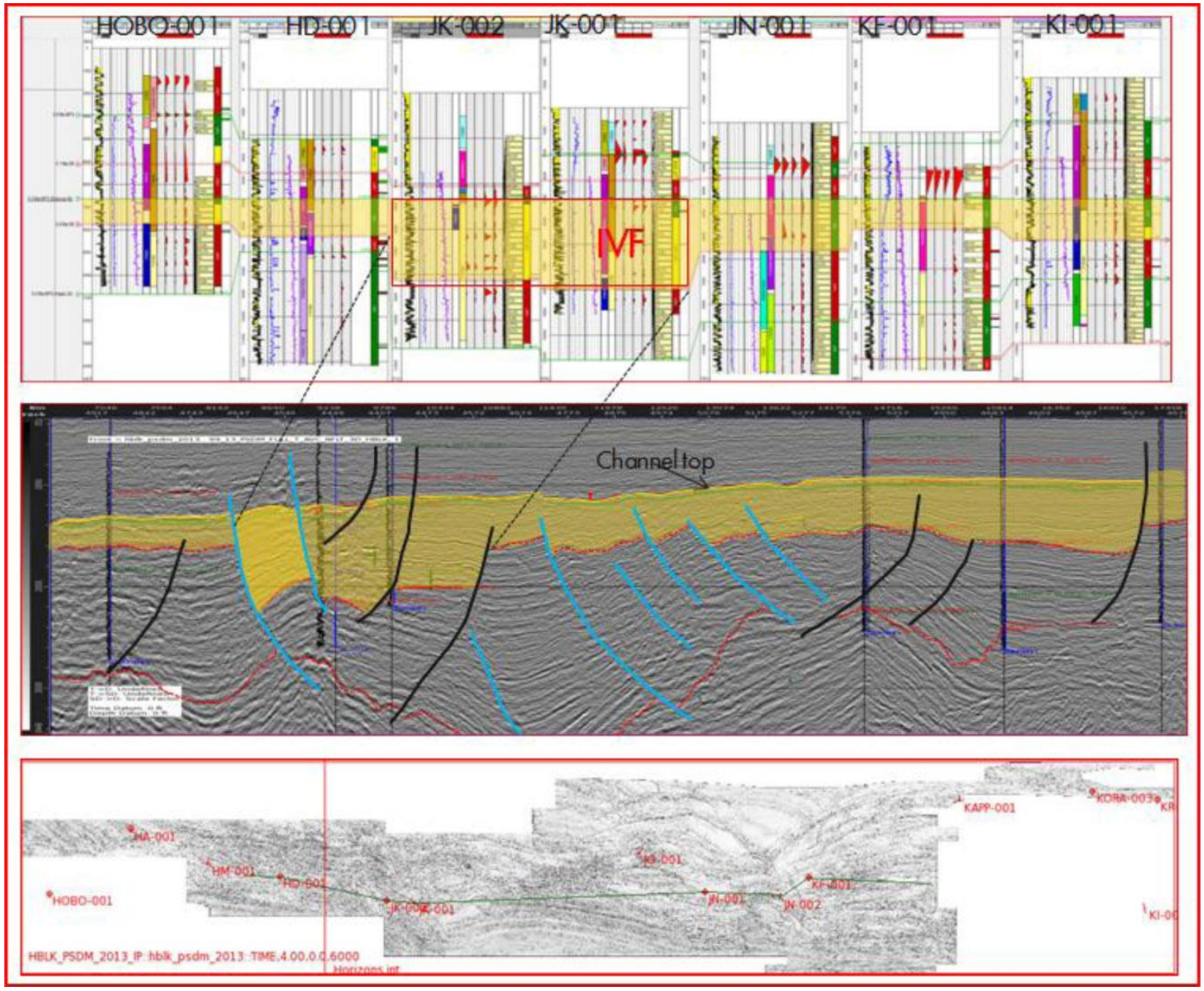

Figure 5. Structural configuration projected onto the flatten surface.

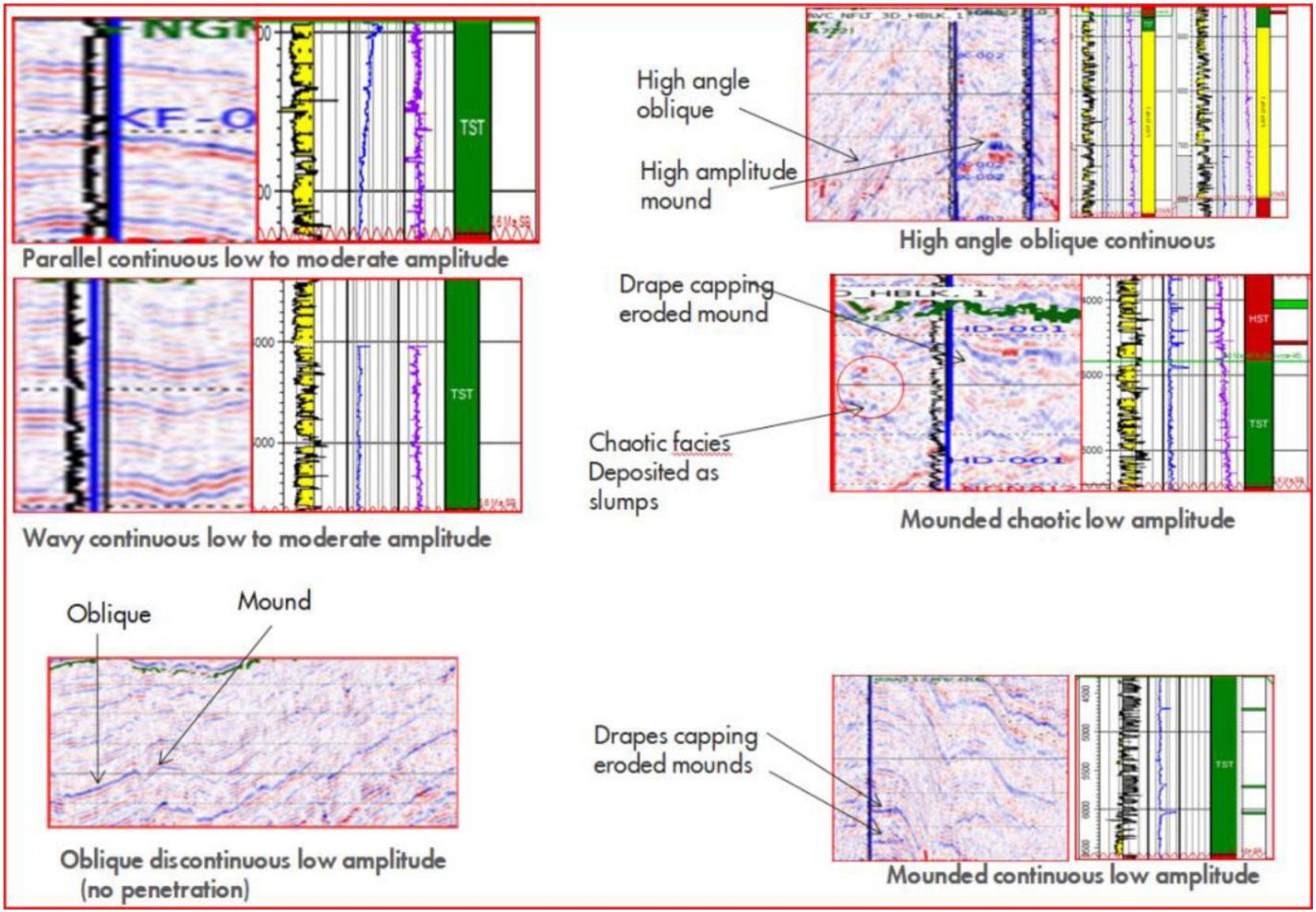

Figure 6. Examples of six interpreted seismic facies.

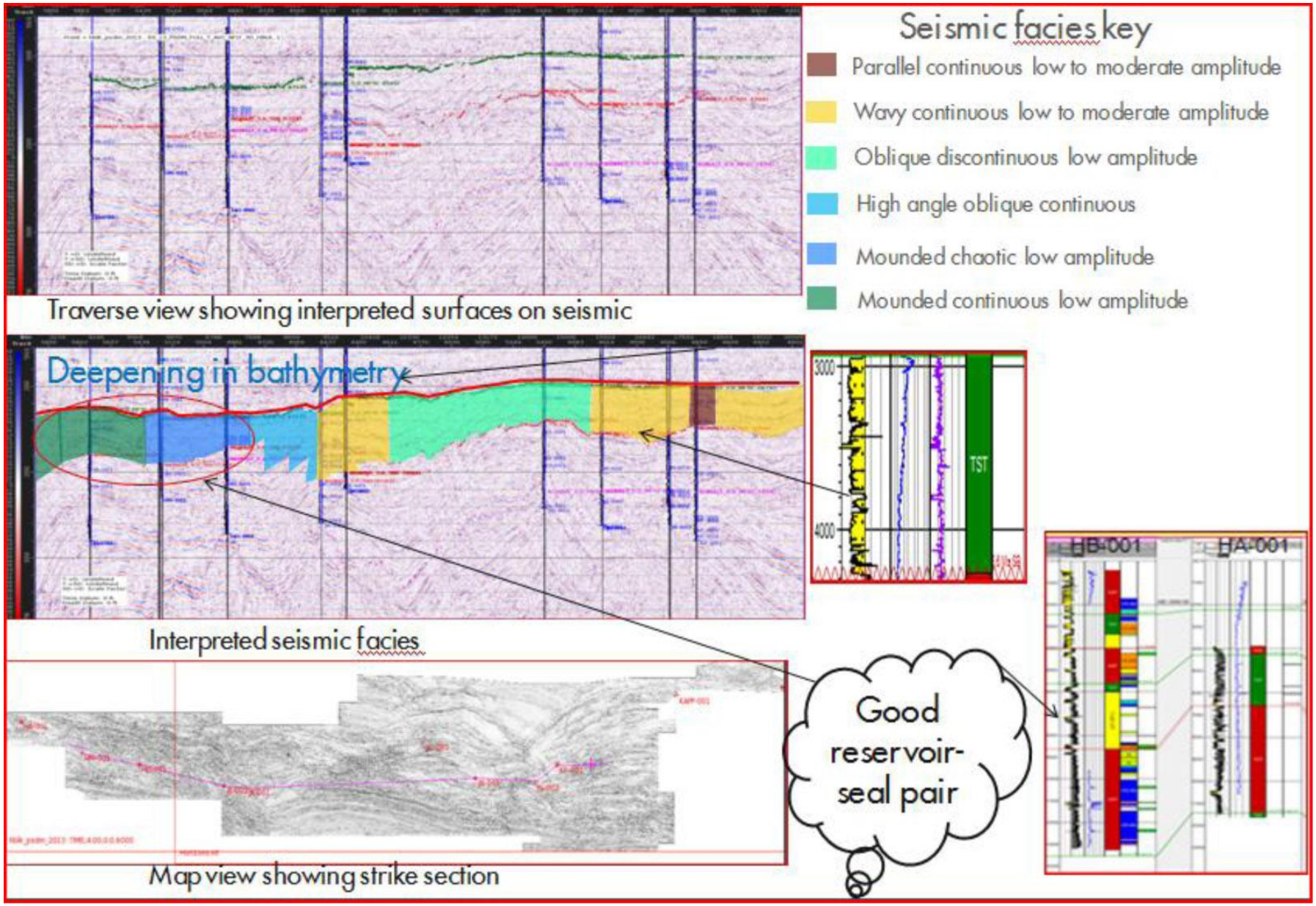

Figure 7. Seismic facies calibrated with well information.

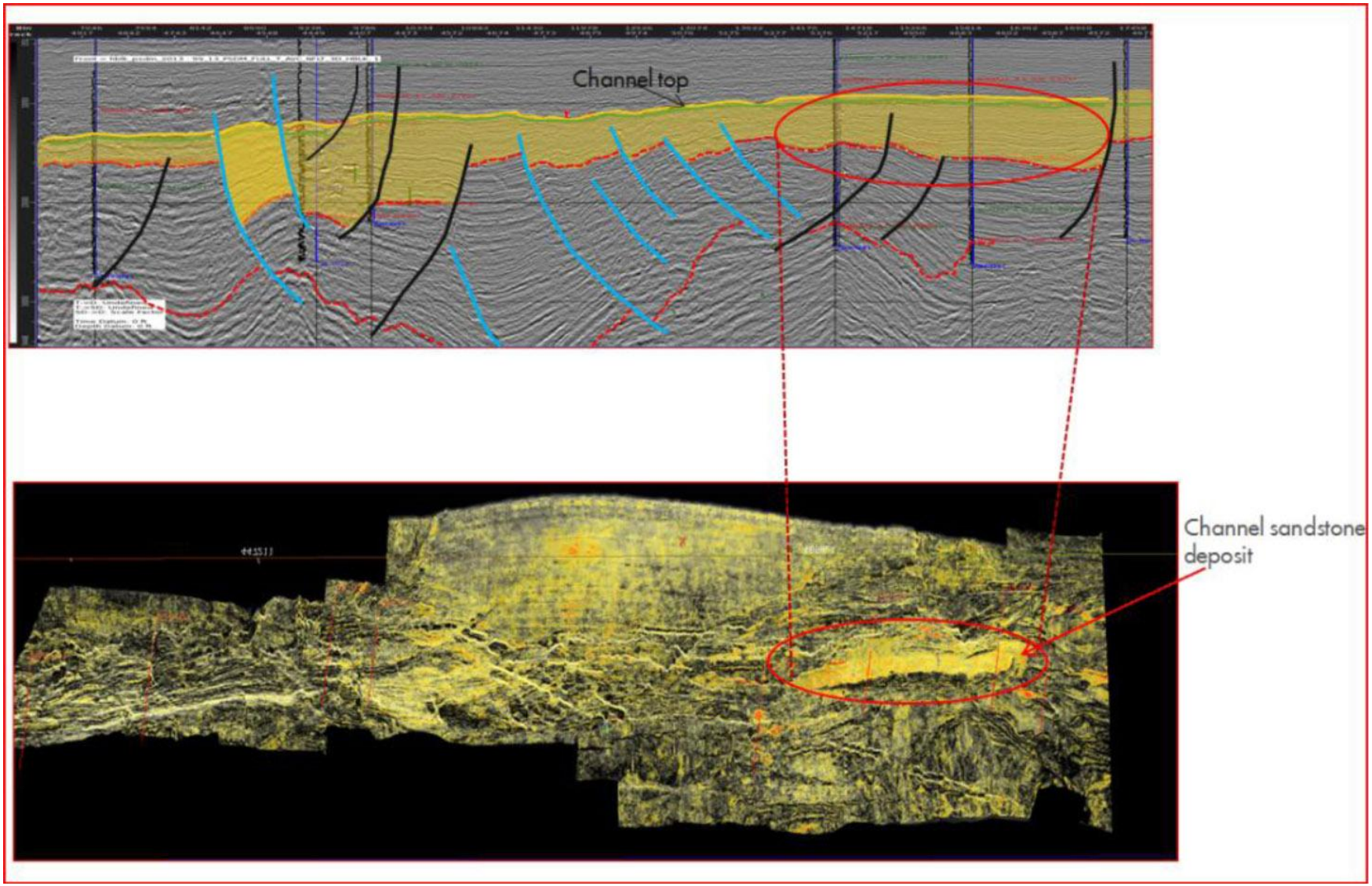

Figure 8. Proportional slicing at 4.0 msecs window.

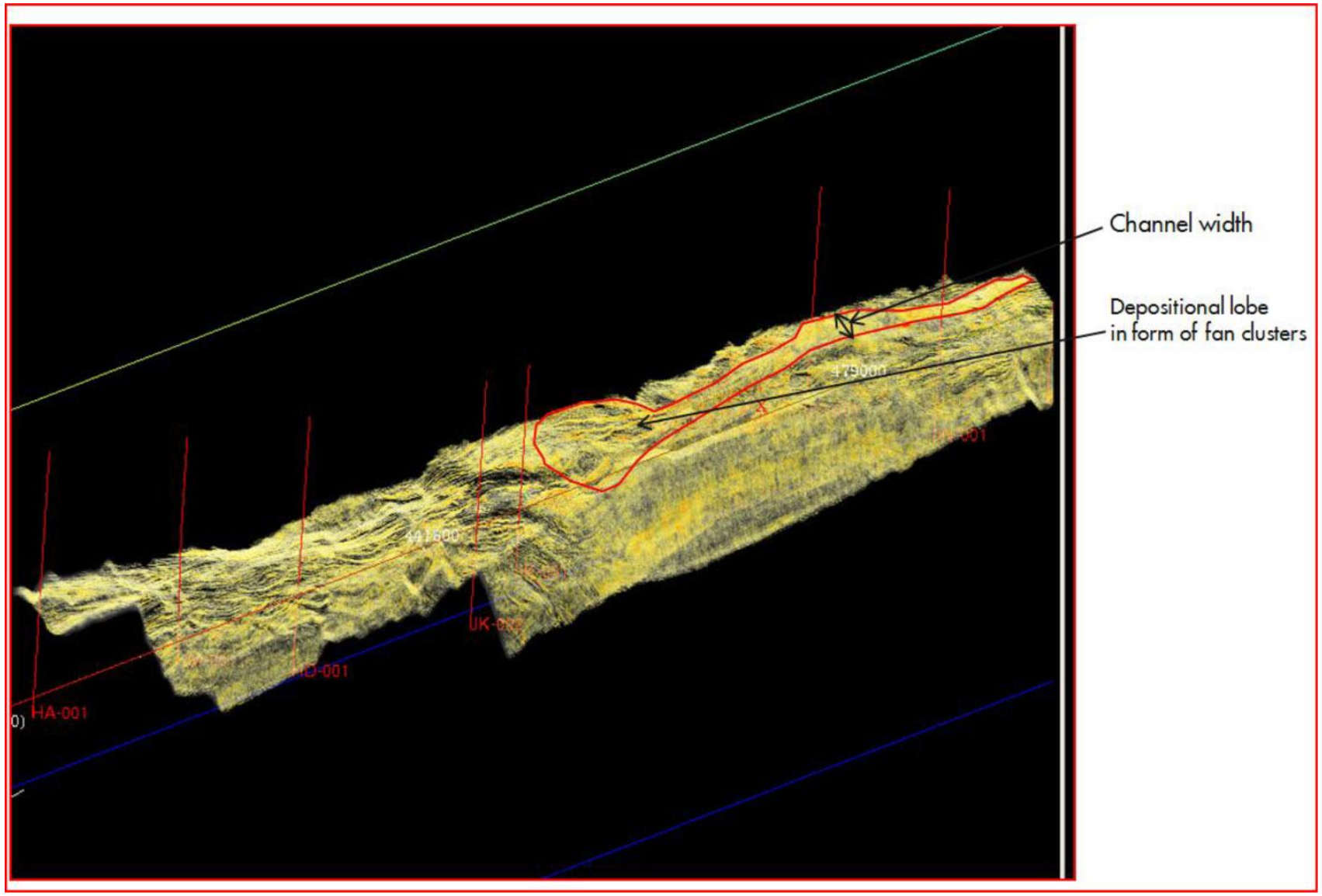

Figure 9. Horizon slicing at 4.4 msecs window.

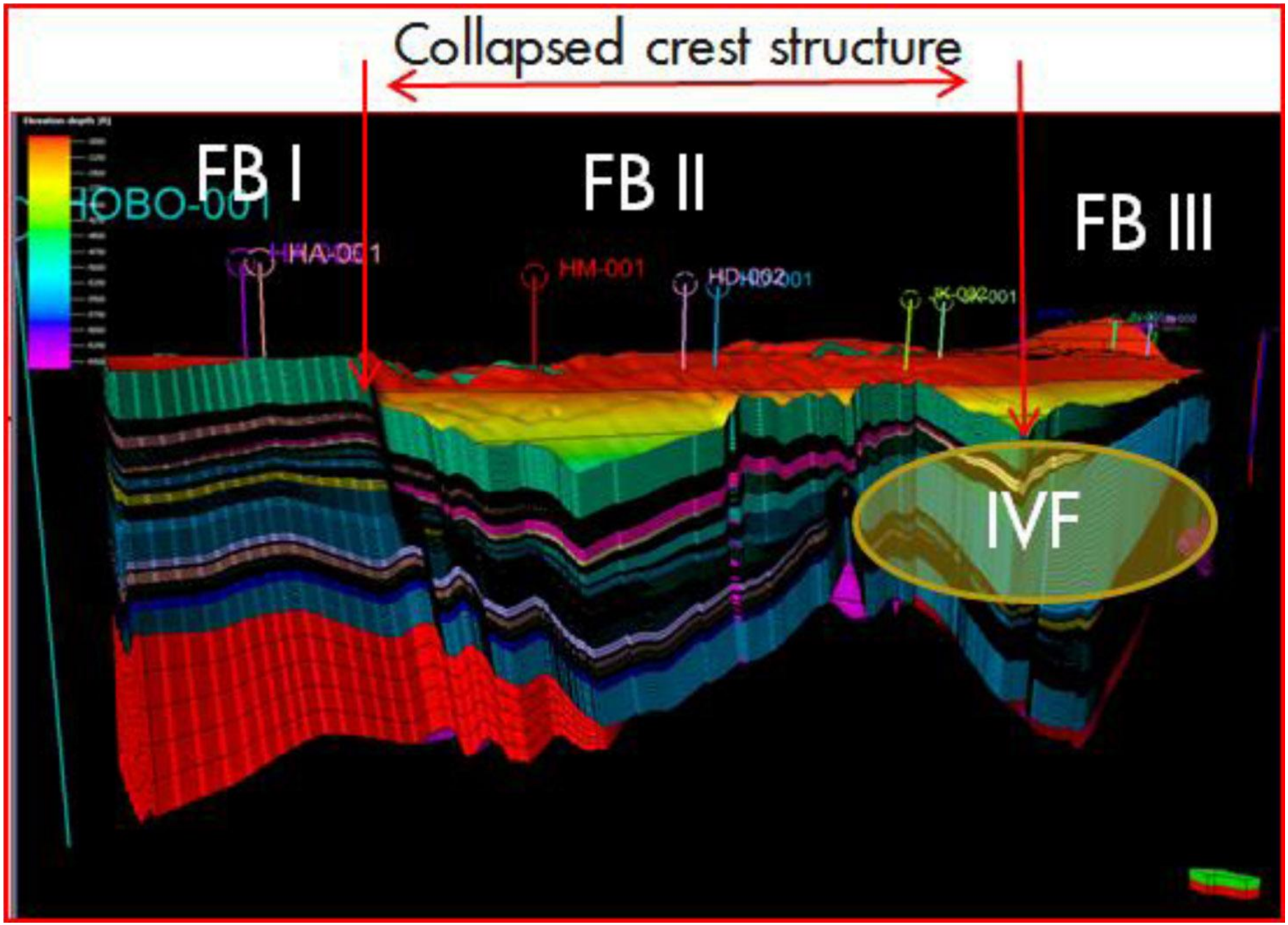

Figure 10. 3-D geologic model.